

THE TIP OF THE RED GIANT BRANCH AS A DISTANCE INDICATOR FOR RESOLVED GALAXIES: II. COMPUTER SIMULATIONS

BARRY F. MADORE

NASA/IPAC Extragalactic Database

Infrared Processing and Analysis Center

California Institute of Technology

Pasadena, California 91125

c-mail: barry@ipac.caltech.edu

and

WENDY L. FREEDMAN

The Observatories

Carnegie Institution of Washington

Pasadena, California 91101

c-mail: wendy@ociw.edu

Received

Accepted

Address for Proofs:

Running Headline: *RED GIANT BRANCH TIP*

Barry F. Madore

NASA/IPAC Extragalactic Database MS 100-22

California Institute of Technology

Pasadena, CA 91125

ABSTRACT

Based on both empirical data for nearby galaxies, and on computer simulations, we show that measuring the position of the tip of the first-ascent red-giant branch (TRGB) provides a means of obtaining the distances to nearby galaxies with a precision and accuracy comparable to using Cepheids and/or RR. Lyrae variables. We present an analysis of synthetic *I* versus (*V-I*) color-magnitude diagrams of Population II systems to investigate the use of the observed discontinuity in the *I*-band luminosity function as a primary distance indicator. In the simulations we quantify the effects of (1) signal-to-noise, (2) crowding, (3) population size, and (4) non-giant-branch-star contamination, on the method adopted for detecting the discontinuity, measuring its luminosity, and estimating its uncertainty. We discuss potential sources of systematic error in the context of observable parameters, such as the signal-to-noise ratio and/or surface brightness. The simulations are then scaled to observed color-magnitude diagrams. It is concluded, that from the ground the tip of the red-giant-branch method can be successfully used to determine distances accurate to $\pm 10\%$ for galaxies out to 3 kpc ($\mu \sim 27.5$ mag); and from space a factor of four further in distance ($\mu \sim 30.5$ mag) can be reached using *HST*. The method can be applied wherever a metal-poor population ($-2.0 < Z < -0.7$) of red-giant stars is detected (whose age is in the range 7–17 G yr), whether that population resides in the halo of a spiral galaxy, the extended outer disk of a dwarf irregular, or in the outer periphery of an elliptical galaxy.

Subject headings: galaxies: distances — stars: Red Giants

1. INTRODUCTION

An empirical demonstration of the precision and accuracy of the magnitude of the tip of the red giant branch (hereafter TRGB) as a primary distance indicator has been given in Lee, Freedman and Madore (1993). These authors applied the technique to a variety of nearby galaxies spanning the entire range of morphological types, from dwarf ellipticals (NGC 147, 185 and 205), to early-type spirals (M31), late-type spirals (M33) and irregulars (NGC 3109, NGC 6822, IC 1613 and WLM). Compiling new and previously published data on the apparent brightness of the number-count discontinuity in the red-giant-branch luminosity function (see references therein), they demonstrated an extremely good correspondence between the moduli for these nearby galaxies (independently derived from Cepheids and/or RR Lyrae stars) with the moduli derived assuming that the bolometric luminosity of the TRGB is a standard candle. Like Cepheids and RR Lyraes, the TRGB method has an underlying physical basis: the tip of the first-ascent red-giant branch represents the luminosity of the core helium flash, which, according to theory (see Iben & Renzini 1983) is essentially constant, having very little sensitivity to metallicity and/or age.

In Lee, Freedman and Madore (1993) an objective edge-detection algorithm, employing a Sobel filter, was applied to this problem for the first time (previously published estimates of the discontinuity having been made either by eye or from arguments relating to the Poisson statistics of the luminosity function.) In the following we present an expanded analysis of the adopted TRGB detection and measurement method, in order to quantify its application to the extragalactic distance scale, and to estimate the distance limit out to which this method can be reasonably applied.

2. THE MODEL

For the purpose of the simulations presented here, a synthetic Population II giant branch was generated based on the color-magnitude diagram of the intermediate-metallicity globular cluster M2, which has a metallicity of $[\text{Fe}/\text{H}] \sim -1.6$. The synthetic giant branch was populated according to a power-law distribution such that $\log(N) = 0.6 \times I$ (where N is the number of stars per I -band magnitude) with a sharp cut-off set at an absolute magnitude of $M_I = -4.00$ mag. Choosing an alternate fiducial sequence (or a combination of different metallicity sequences) would not substantially alter the results presented since within the range of interest, $-2.2 < [\text{Fe}/\text{H}] < -0.7$, the discontinuity in the I -band magnitude is quite insensitive to metallicity, as illustrated in Figure 1 of LCC, Freedman and Madore (1993). However, it should be emphasized that this method cannot be extended to greater metallicities where line blanketing becomes significant even in the I band.

Four parameters were independently varied in the simulations: (1) the number of detected photons (or equivalently the photon-count signal-to-noise ratio, SNR) for the stars defining the TRGB (with the counts for stars fainter than the tip being scaled accordingly), (2) the crowding, expressed as the amount of contamination of the stellar photometry due to unresolved multiple stellar images within a given point spread function (which are either due to accidental contamination or intrinsic duplicity), (3) a population scaling factor, expressed as the total number of stars found in the upper three magnitudes of the red giant branch, and finally (4) the foreground/background contamination of stellar images contributed by non-giant-branch stars. As discussed in Section 3.4 there are several potential sources of contamination, all of which result in a reduction in the contrast of the jump in the luminosity function at the TRGB.

The model generates discrete numbers of stars with luminosities calculated to 0.01 mag. These data are then collected into 0.10 mag bins, which, as for the actual data, are small enough so that they do not dominate the error in detecting the TRGB discontinuity, but are large enough that reasonable

numbers of stars can be expected to contribute to the counting statistics associated with each bin, Our aim is to test the limitations on defining the '1 RGB to better than *0.2 mag (that is $\pm 10\%$ in distance).

2.1 The Edge-Detection Algorithm

As first introduced in Lee, Freedman and Madore (1993), we have adopted here a standard image-processing edge-detection technique to measure the luminosity of the onset of the RGB. The kernel $[-1, 0, +1]$, known as a Sobel filter (e.g., Myler & Wilkes 1993) produces an output that reflects the gradient detected across a three-point interval. It is a first-derivative operator which computes the rate of change across an edge. Figure 1 shows the idealized output of such a filter for a series of idealized possibilities. A simple discontinuity (top panel) results in a sharp spike in the filter output. An abrupt, but continuous, change of slope (middle panel) results in the output discontinuously changing its level. Taken in combination, (bottom panel) a change in slope occurring after an abrupt discontinuity y (as is expected in an idealized TRGB luminosity function) results in the output shown in the third panel: an abrupt spike, marking the discontinuity, followed by a plateau, marking the new value of the slope.

At low signal-to-noise ratios (i.e., low photon count rates) the primary spike registered at the discontinuity will be degraded, and noise will also enter the baseline leading up to the edge. Although distinctive in their $[+1, -1]$ response to the Sobel filter function (see the bottom panel] of Figure 1), noise spikes can be a source of confusion in practically identifying the onset of the TRGB for small populations. Accordingly, we also investigated the use of an extended Sobel filter, which we have devised, incorporating a weighted kernel, covering a wider baseline: $[-1, -2, 0, +2, +1]$. This filter again responds to gradients but it is more resilient to isolated noise spikes, by effectively smoothing over a larger number of cells.

3. THE SIMULATIONS

Using our discrete-star model for the TRGB and applying the edge-detection software, described above, we proceed in the following sections to investigate the effects of major sources of errors (both random and systematic) in the determination of the luminosity of the TRGB for distance determinations.

3.1 *Signal-to-Noise Ratio*

In this section we begin by considering the case where photon-counting statistics are the dominant source of error in the signal-to-noise ratio (SNR) for the measured magnitudes of isolated stars. The SNR is parameterized through an equivalent number of photons, N_T , for a star at the TRGB, giving $SNR_{TRGB} = N_T / \sqrt{N_T}$. Errors in the magnitudes for other stars were scaled by luminosity from this starting value.

The top panel in Figure 2 shows the luminosity function resulting from a simulation where the SNR was high (70) at the TRGB, resulting in a well-defined red-giant branch (middle panel) and a highly confident measure of the luminosity of the discontinuity, as shown by the Sobel filter output given in the bottom panel of Figure 2.

Naturally, as the photometric errors increase the sharpness of the TRGB discontinuity decreases, and the random photometric errors slowly give rise to a systematic error in the derived position of the jump. The effect is shown in Figure 3. Here the results of a number of simulations, with no crowding and no field contamination, are given, varying only the photon statistics in the stellar photometry. The diagram can be used to provide a simple prescription for a minimum SNR required to keep this particular systematic error below some preselected level. For instance, if a systematic error (due to this effect) is required to be less than 0.10 mag, then one should best keep the SNR greater than 5. An example of a case where $SNR = 10$ is given in Figure 4.

3.2 Crowding

The effects of crowding were simulated by appropriately combining the intensities of stars chosen at random from the luminosity function interval spanning the first three magnitudes below the '1'RGII. (Since the major effect on the TRGB is due to chance combinations of stars intrinsically near to the discontinuity, working deeper into the luminosity function simply increases the computation time without substantially altering the effects on the bright end.) The procedure was as follows: A crowding rate, expressed as a percentage, was chosen. Two stars were then randomly selected from the upper three magnitudes of the RGB luminosity function. The luminosity of the fainter star was added to the brighter; and the fainter star was deleted from the list. The process was repeated, taking care not to allow the same star to be accidentally added to itself, while at the same time not disallowing previously combined stars to be further contaminated on subsequent rounds. Iteration stopped when the input percentage of stars crowded was reached. It should be noted here that by this definition a crowding rate of N means that $N\%$ of the population is chosen to be combined with another $N\%$ resulting in an observed percentage of stars, that are in fact composite, equivalent to $N/(100 - N)$.

Figure 5 shows the effect of 10% crowding on a well-populated luminosity function, at high (31) SNR. The shift in the discontinuity, as expected, is systematic, being brighter by ~ 0.15 mag in this instance. A series of simulations involving 13,000 stars in the upper three magnitudes of the luminosity function were run for a variety of crowding rates to further quantify the drift in the measured luminosity of the TRGB as a function of crowding. The results are shown in Figure 6. As can be seen, the systematic off-set can be kept below ~ 0.2 mag for crowding rates less than about 25% (that is, one star out of every three measured is contaminated by another star at most three magnitudes fainter than the TRGB). Not only does the measured TRGB drift to brighter magnitudes but the discontinuity softens (as shown by the magnitude error bars attached to the data in Figure 6) such that the uncertainty in measuring the (biased) magnitude of the jump is itself almost as large as the offset.

If one is interested in keeping both the systematic and random errors in applying this method at or below the 10%-in-distance level, the superimposed random errors will limit this method to situations where the crowding rates are assessed to be less than 25%.

3.3 *Population Size*

Of all of the effects considered in this simulation, population size is the only effect that can result in an over-estimate of the apparent distance modulus. This effect occurs only when the total population of the RGB is so small that small-number statistics result in the upper-most bins being empty, creating the impression of a fainter tip. Of course any luminosity function where the first observed bin contains only one star should be viewed with caution, especially if the subsequent bins merely fill at the expected power-law rate. To confidently identify the TRGB discontinuity the luminosity function needs to be well-populated.

We have parameterized the population size by the number of stars in the first full magnitude of the luminosity function as measured from the intrinsic TRGB. The application of the edge-detection algorithm (using a binning interval of 0.1 mag and saw-tooth smoothing the edge-detector over 5 bins) indicates that the systematic effects of depopulating the bin defining the tip do not produce a systematic effect until fewer than 50 stars are measured in the upper magnitude interval. Until that point almost all of the (high SN R) solutions fall within one standard deviation of the true value, and furthermore those internal errors are all significantly less than 0.1 mag.

Thus, if approximately 100 stars can be imaged in the first magnitude interval, the luminosity function will be sufficiently filled to define the discontinuity limited solely by other effects.

3.4 Field Contamination

As mentioned previously, any contamination of the observed luminosity function, whatever its source, will lead to a decrease in the effective contrast in the TRGB discontinuity (see Figure 8, for example.) To parameterize this effect we computed an effective SN R corresponding to the ratio of the number of RGB stars to the number of field objects in the first magnitude interval below the TRGB. We added a uniformly distributed background population into the color-magnitude diagram, reconstructed the apparent luminosity function and applied the edge detector.

Statistical noise in the field luminosity function produces a background of false signals as the edge detector moves toward the TRGB. It is against this noise that the signal of the TRGB discontinuity must be measured. A grid of models having well saturated RGB luminosity functions embedded in various amounts of background contamination yields the following conclusions: As long as the SN R associated with the crowding exceeds 5:1 the significance of the true discontinuity (as measured by the Sobel filter output amplitude) is at least three sigma. The background noise output of the Sobel filter can be reduced without much effect on the true discontinuity by increasing the filter band width. However, since the background contamination, if considered significant, can be corrected for statistically (by observing off-galaxy fields) we did not explore changes in the filter function any further.

For even the nearest elliptical galaxies whose distances might be explored by these techniques the number of high-latitude Galactic foreground stars with an apparent magnitude in excess of $I > 21$ mag is totally negligible over the area of interest centered on the galaxy itself (a few square arcmin at most; see, for example, Bahcall and Soneira 1981). If the TRGB is detected at the level demanded by the population criterion discussed in the previous section (i.e., at least 100 stars in the first magnitude interval) then it is clear that a SN R in excess of 3 will be guaranteed in the present context of foreground contamination.

For spiral galaxies where the primary contamination is not Galactic, but rather intrinsic to the

parent galaxy itself, the youngest population supergiants can in principle be eliminated by color discrimination using an additional exposure to produce a color-magnitude diagram. Alternatively, moving as far into the halo (and as far away from the disk out) as is possible would be more efficient, and avoids the problem in the first place.

Other sources of contamination noise may be present (background galaxies, globular clusters, and quasars, etc.), but the dominant concern is the potential presence of an extended asymptotic giant branch (AGB) population. Most background galaxies will be resolved. Globular clusters in the parent galaxy will be far brighter than the individual giants at the TRGB, and therefore of no direct consequence in detecting the discontinuity. And background quasars will contribute only a small signal occasionally. AGB stars originating from intermediate-aged populations in spiral (and even some elliptical) galaxies can overlay the RGB and may contribute significantly to the observed luminosity function. Being systematically brighter than the RGB at all colors, the extended AGB can distort or displace the discontinuity in the luminosity function due to the TRGB. Again, avoidance is the best prevention. Working in the outer extremities of either spiral halos or elliptical envelopes, a significant population of intermediate-aged stars contaminating the counts is unlikely..

4. CALIBRATING THE SIMULATIONS: HOW FAR CAN THE TRGB BE RELIABLY APPLIED?

To be of any practical use the computer simulations presented above need to be interfaced to real data. We have chosen to use the data published by Lee (1993) on the TRGB in the galaxy NGC 3109. This galaxy is situated at a distance of about 1.25 Mpc (i.e., a true distance modulus of 25.4 mag). Lee's I-band luminosity function for the RGB was based on an accumulated exposure of 2,400 sec taken in moderate (1.1 arcsec) seeing using the duPont 2.5m telescope. The area on the sky covered by his outer field was approximately 10,000 seeing/resolution elements; and in the first magnitude interval below the TRGB Lee found 125 stars. For scaling purposes, using our model of the RGB luminosity function Lee's number for the first magnitude bin (after which he is seriously incomplete) predicts a total of 3,200 stars are contained in the first three magnitudes below the TRGB.

We have produced a poisson simulation of the areal crowding associated with this observation, and calculate that, as observed from the ground at this given seeing and surface brightness in NGC 3109 ($B = 26.0$ mag/square arcsec according to Carignan 1985), 27% of Lee's objects are expected to be multiple (in the sense defined by Section 3.2). Figure 5 then indicates that Lee's value of the TRGB magnitude is probably overestimated by -0.2 mag due to a crowding-induced brightening. Further observations at higher spatial resolution can readily test this conclusion.

We can now scale these results to other distances. Here we simply consider an increase by a factor of ten in distance above that of NGC 3109 (i.e., to a true modulus of 30.4 mag, or 12 Mpc). If observed from the ground (with one arcsec seeing) the TRGB stars in a galaxy this distant would be unacceptably crowded, at the surface brightness level where Lee (1993) observed NGC 3109. However, using the *Hubble Space Telescope* at its diffraction limit of 0.1 arcsec would exactly off-set this distance-induced (factor of 10) effect. That is, one could observe from space at $B = 26$ mag/square-arcsec and suffer no more crowding errors than are already being incurred in the NGC 3109 observations.

A crowding factor of 27% is only marginally acceptable if a 10% error in derived distance (0.2 mag in the distance modulus) is desired. However, for a fixed detector size, a factor of ten increase in target distance increases the area (and therefore the number of stars surveyed) by a factor of 100. In principle, one could then work at a surface brightness level 100 times fainter without violating the population size minimum criterion (that is, 50-100 stars in the first magnitude interval below the TRGB) for a statistically reliable measure of the TRGB discontinuity (Section 3.3). The situation is even more favorable when comparing and scaling the Lee (1993) data to the capabilities of the HST WFPC2: since HST has three (800 x 800 pixel) chips, and the entire surface of each chip can be used (as opposed to the Lee data where only one fifth of a 500 x 500 pixel chip was used). Thus there is an additional cumulative advantage of about a factor of 35x in population detected, in using HST. The factor of two or three lost by moving out to a lower surface brightness level to decrease the crowding effects (i. e., $B = 27 \text{ mag/arcsec}^2$) is completely compensated for by the increased effective areal coverage.

We can now calculate the exposure time required by HST to produce a ten-percent distance estimate, for the above case of a distance a factor of ten further than the NGC 3109 example. Tables 6.1-6.3 and formulae in *WFPC-2 instrument Handbook Version 1.0 MacKenty et al. (1993)* indicate that it is expected that HST will provide a SNR of 17 in the I-band at 26.5 mag given a 3,000 sec exposure. We therefore conclude that a distance modulus of 31 mag (i.e., Virgo) is quite feasible using this technique with reasonable exposure times using HST, in fact a modulus 3 mag fainter (i. e., 60 Mpc in distance) is possible if a limiting SNR = 4 were to be adopted.

Finally, we estimate directly from the published data just how far this technique might reasonably be applied from the ground. For a minimum acceptable SNR of 4 the Lee (1993) data indicate that $I_{\text{max}} \sim 23.5 \text{ mag}$. Adopting $M_I = -4.0 \text{ mag}$ for the TRGB discontinuity, this limiting magnitude corresponds to a true distance modulus limit, of 27.5 (or distances just in excess of 3 Mpc). This goes well beyond the Local Group and encompasses dozens of galaxies associated with the M81-NGC2403-IC342 and

SouthPolar Groups of galaxies, for instance. A systematic survey of the distances to these individual objects is well within the grasp of ground-based telescopes with good seeing (better than one arcsec) and moderate aperture (greater than 2.5m). Such a survey is now underway at Palomar and at the Las Campanas Observatory.

5. SUMMARY and CONCLUSIONS

Distances measured using the tip of the red giant branch for metal-poor stars were found empirically by I, MF93 to be comparable in precision to those distances derived from Cepheids and RR Lyrae variables. In this paper, the limits of this technique have been explored and quantified by computer simulation. Four effects were modeled: photometric errors, crowding, population size and contamination. From the simulations we draw the following conclusions.

(1) Photometric errors both smooth out the TRGB discontinuity, and systematically shift the inferred position of the discontinuity to brighter magnitudes (see Section 3.1). The shift occurs because while the errors for individual stars are symmetric in sign, the edge, as identified by its mid-point, is an asymmetric feature. That feature then can only move systematically to brighter magnitudes as the random error in the stellar photometry increases. For $\text{SNR} > 5$ the systematic error in measuring the tip is generally kept below 10% in the distance estimate; but thereafter it is a rapidly deteriorating function of decreasing SNR. *This limitation sets the minimum required integration time (for a given telescope) as a function of distance.*

(2) Crowding, as expected raises stars to brighter magnitudes and also erodes any sharp features in the luminosity function. Crowding systematically affects the definition of the edge of the TRGB such that if more than 2570 of the stars in the first three magnitudes of the giant-branch luminosity function are multiple, then the derived distances will be systematically in error by more than 10%. *This criterion sets an upper limit on the surface brightness level that can be worked on at a given distance and a given resolution.*

(3) Population Size. At any given SNR, the population size must exceed a critical amount so that the discontinuity is adequately defined, by having at least one member in the first bin. For the bin size and edge-detection kernel used here, it was found that the systematic error remained below 0.1 mag until fewer than 50 stars were measured in the brightest magnitude interval. This criterion sets a lower limit on the physical area that must be surveyed at a given surface brightness.

(4) Background/Foreground Contamination. in any composite population and for most lines of sight there will be stars populating the color-magnitude diagram that have a comparable apparent brightness, but do not in fact belong to the giant-branch population being investigated. For composite systems (such as spiral galaxies, or ellipticals with evidence for a recent bursts of star formation) working as far out into the halo as possible has obvious merit. Furthermore, working far out in the halo both ensures a low-metallicity population (which is required for this technique to be applicable) and at the same time works toward minimizing crowding/confusion errors.

Scaling the simulations to published observations made with ground-based telescopes and comparing with tabulated performance characteristics for HST, the discontinuity in the luminosity function at tip of the red giant branch can be expected to be used as a precision distance indicator out to at least 3 Mpc using ground-based telescopes at sites with reasonably good seeing, while distances out to ~13 Mpc can be expected to be reached with HST using modest (~1 hour) exposure times.

Acknowledgements

BFM would like to especially thank Jim Schombert for the generous sharing of his time and software in this and other scientific undertakings over the years. BFM was supported in part by the NASA/IPAC Extragalactic Database (NED) and the Jet Propulsion Laboratory, California Institute of Technology, under the sponsorship of the Astrophysics Division of NASA's Office of Space Science and Applications. This work was partially funded by NSF Grant No. AST 91-16496 to WLF, and made use of the on-line services of NED.

References

- Bahcall, J.N. & Soniera, R.M. 1981, ApJ, 47, 337
- Carignan, C. 1985, ApJ, 299, 59
- Iben, I. & Renzini, A. 1983, ARAA, 21, 271
- Lee, M.G. 1993, ApJ, 408, 409
- Lee, M. G., Freedman, W. L., & Madore, B. 1993, ApJ, 417, 553
- Myler, J. R. & Weekes, A. R. 1993, *Computer Imaging Recipes in C*, Prentice Hall: N. J.
- MacKenty *et al.* (1993) *WFPC2 instrument Handbook, Version 1.0*, Space Telescope Science Institute,

Figure Captions

Fig. 1 – Idealized response of the Sobel edge-detection filter to a selected combination of slope changes and discontinuities, as described in the text. The bottom panel shows the filter response to an impulse function on input. Note the distinctive positive/negative s-wave without any net change in the mean level in crossing such a disturbance, in contrast to the spike followed by a positive baseline off-set seen in the third panel.

Fig. 2 – *Tip of the Red Giant Branch Simulations* The middle panel shows the simulated I versus $(V-I)$ color-magnitude diagram for a red giant branch having the discontinuity in its luminosity function at $I = -4.0$ mag and $(V-I) = 1.8$ mag (marked by the two horizontal lines). All of the spread in the data shown here is due photon-statistical noise. The upper panel shows the differential luminosity function constructed for the stars in CM diagram but without any color discrimination. Vertical error bars are \sqrt{N} counting statistics; horizontal error bars give the bin size. The dashed vertical line marks the magnitude ($I = -4.0$ mag) at which the discontinuity in the RGB luminosity function is defined. The lower panel shows the output of the 2-point and 4-point Sobel edge-detection filters as applied to the luminosity function in the middle panel. The vertical line again marks the position of the TRGB discontinuity as input. Note the change in level of the filter output after passing through the discontinuity, which corresponds to the changed slope of the luminosity function (from an effectively flat distribution in the field, to a slope of $+0.6$ along the RGB).

Fig. 3- The systematic effects of photometric errors (expressed as a signal-to-noise ratio) on the derived magnitude for the J-band discontinuity in the RGB luminosity function. Each data point is a separate simulation for a large population, with no crowding and zero field contamination. Error bars are the one-sigma widths of a Gaussian fit to the edge-detection output response.

Fig. 4 - The same as Figure 2, with the following exceptions: The SNR depicted here is 10 at the TRGB, and field contamination has been set to zero. In the upper panel, the effects of photometric

errors can be seen to erode the discontinuity by spilling stars into the higher luminosity bins. The lower panel shows how the edge detector has responded to this spill-over in determining a slightly brightened (i.e., biased) estimate of the onset of the TRGB.

Fig. 5- The same as Figure 2, except that the SNR at the TRGB is now 31, and the crowding (as defined in the text) is 10%. A slight field contamination contributes to the noise in advance of the true discontinuity detected at 1.95. Compare with the CMD given in Fig 3b of Lee (1993).

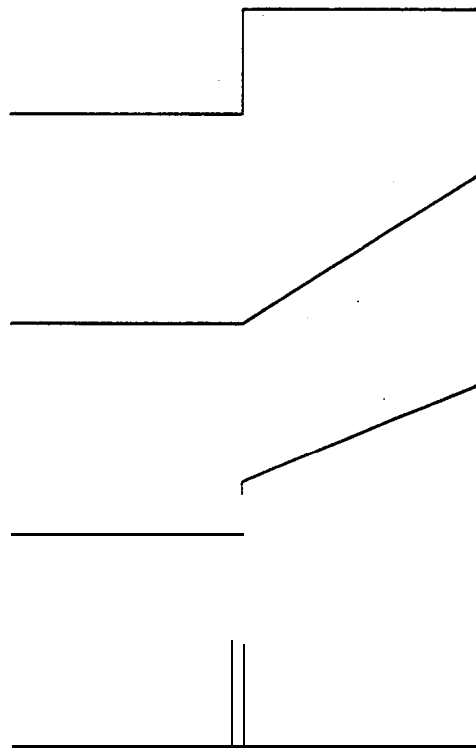
Fig. 6 – The systematic effects of crowding (parameterized by the percentage of stars combined into separate images as drawn from the first three magnitudes of the luminosity function below the TRGB). Each data point is a separate simulation for a large population of high SNR observations, and zero field contamination. Error bars are the one-sigma widths of a Gaussian fit to the cclgc-detection output response.

Fig. 7 – The systematic effects of population size (as expressed as the logarithm of the number of stars in the first magnitude interval below the TRGB) on the derived magnitude for the I-band discontinuity in the RGB luminosity function. Each data point is a separate simulation at high SNR for the photometry, with no crowding and zero field contamination. Error bars are the one-sigma widths of a Gaussian fit to the edge-detection output response.

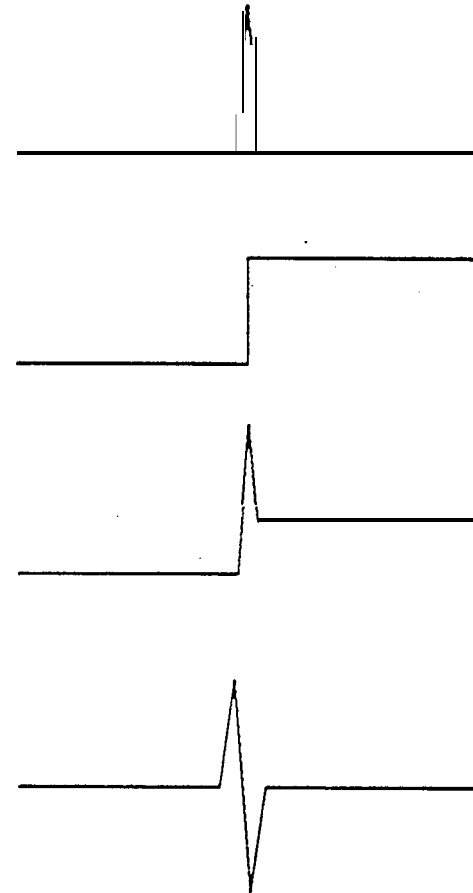
Fig. 8 – The same as Figure 5, except that the crowding has been set to 0% and the field contamination has been elevated to 20 stars per magnitude interval.

Sobel Filter Response

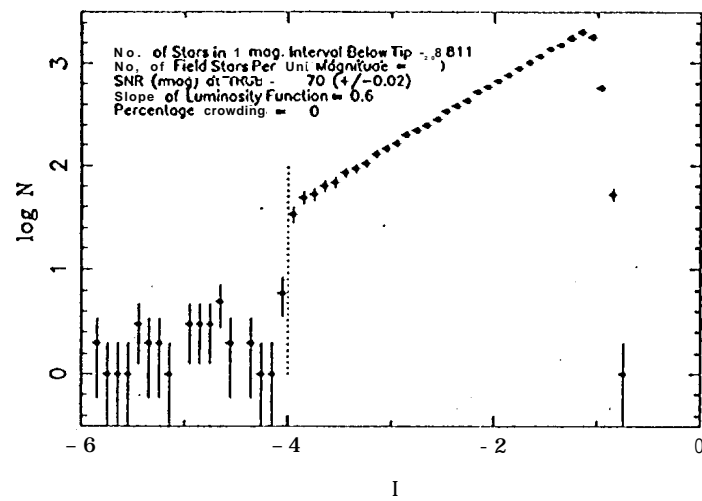
Input Feature



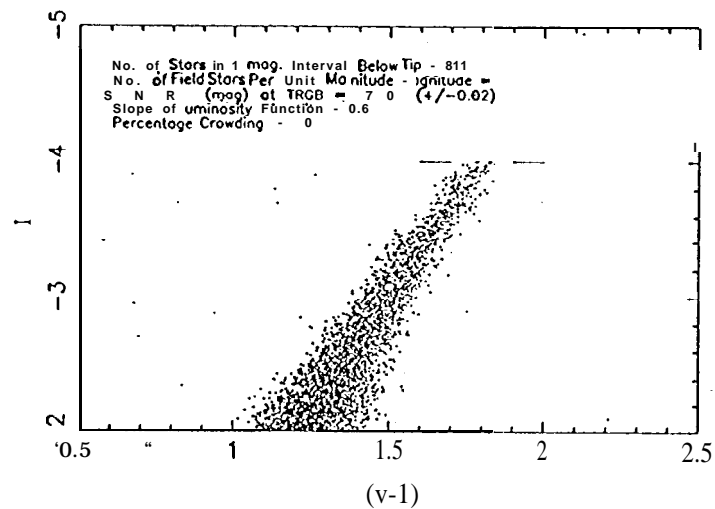
Sobel Filter Output



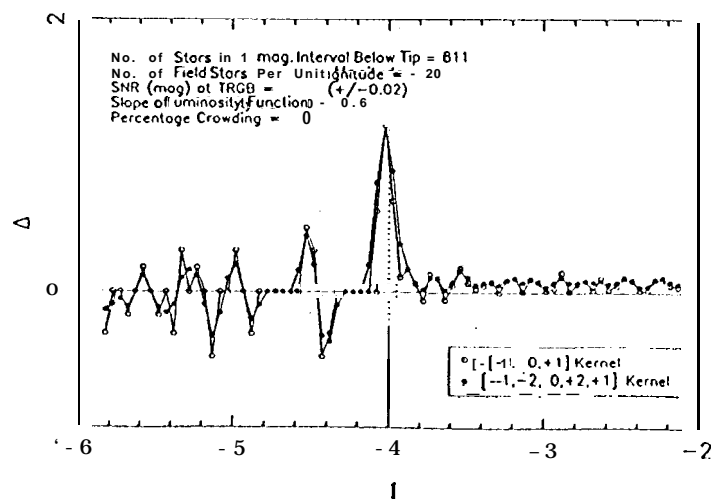
1-Band Red-Giant-Branch Luminosity Function



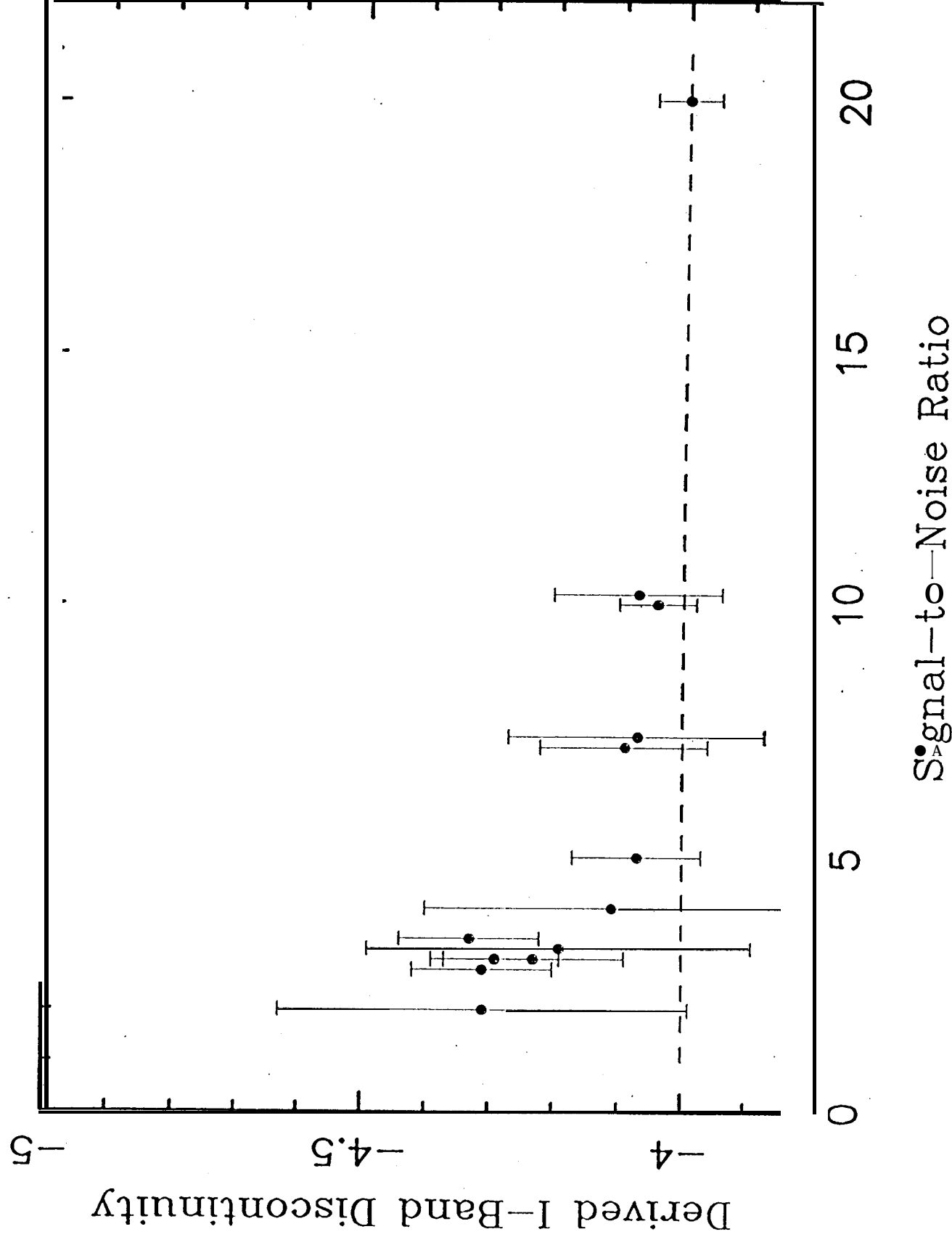
Red-Giant-Branch Color-Magnitude Diagram



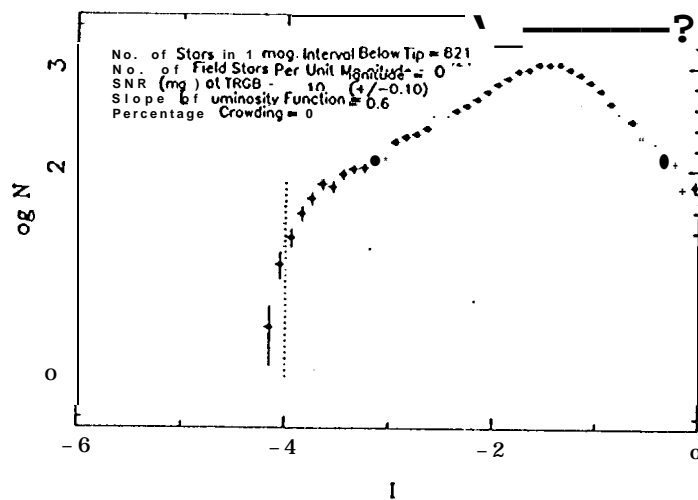
Edge Detection (2- and 4-Point Sobel Kernels)



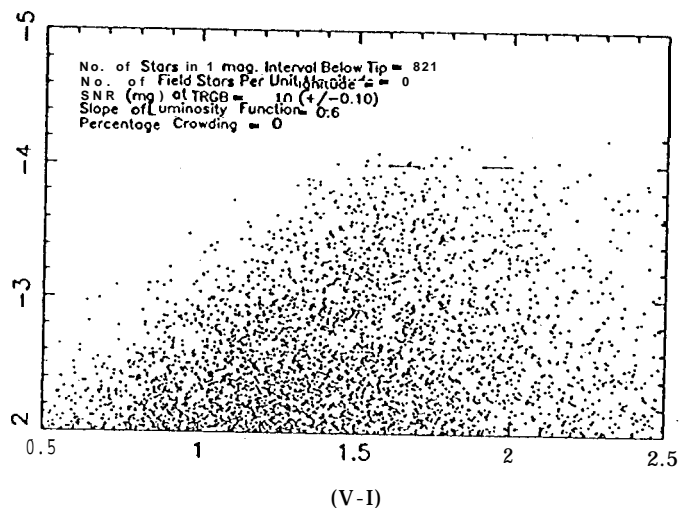
Systematic Effects of Photometric Errors



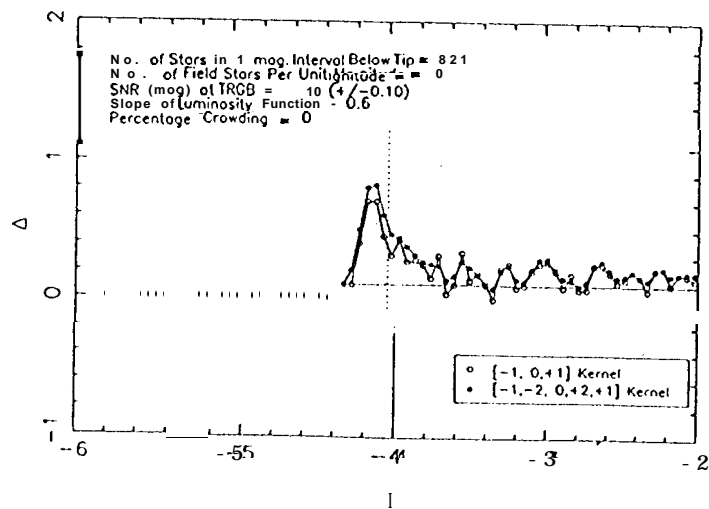
1-Band Red- Giant-Branch Luminosity Function



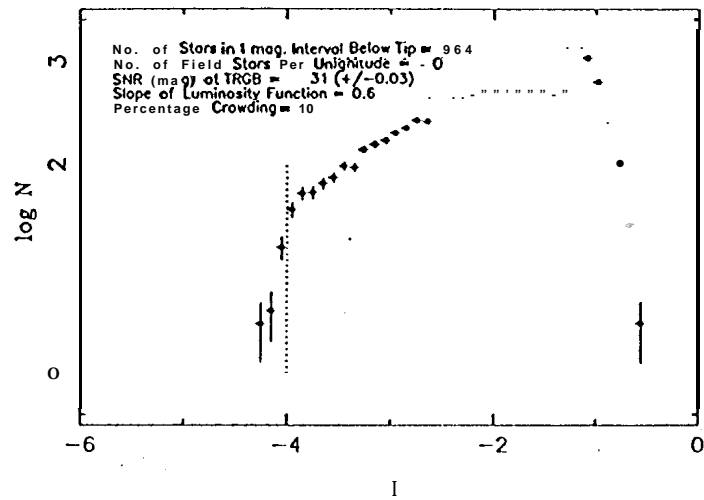
Red-Giant-Branch Color-Magnitude Diagram



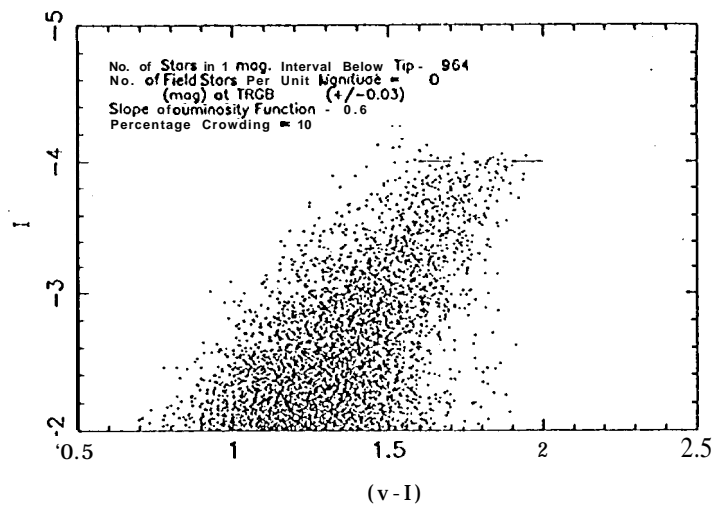
Edge Detection (2- and 4-Point Sobel Kernels)



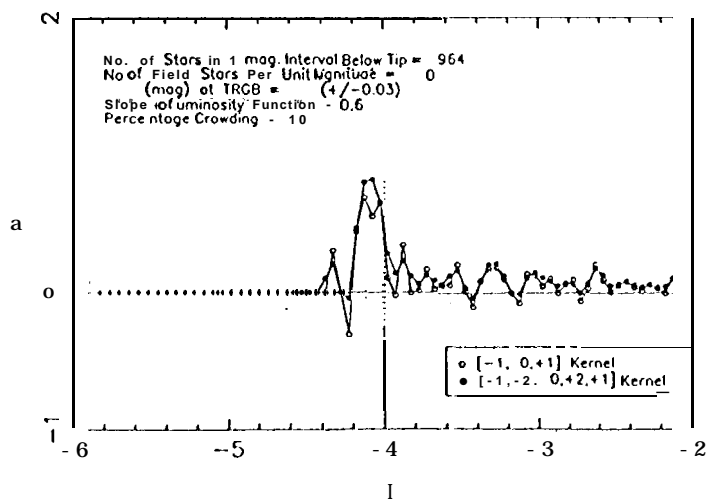
I-Band Red-Giant-Branch Luminosity Function



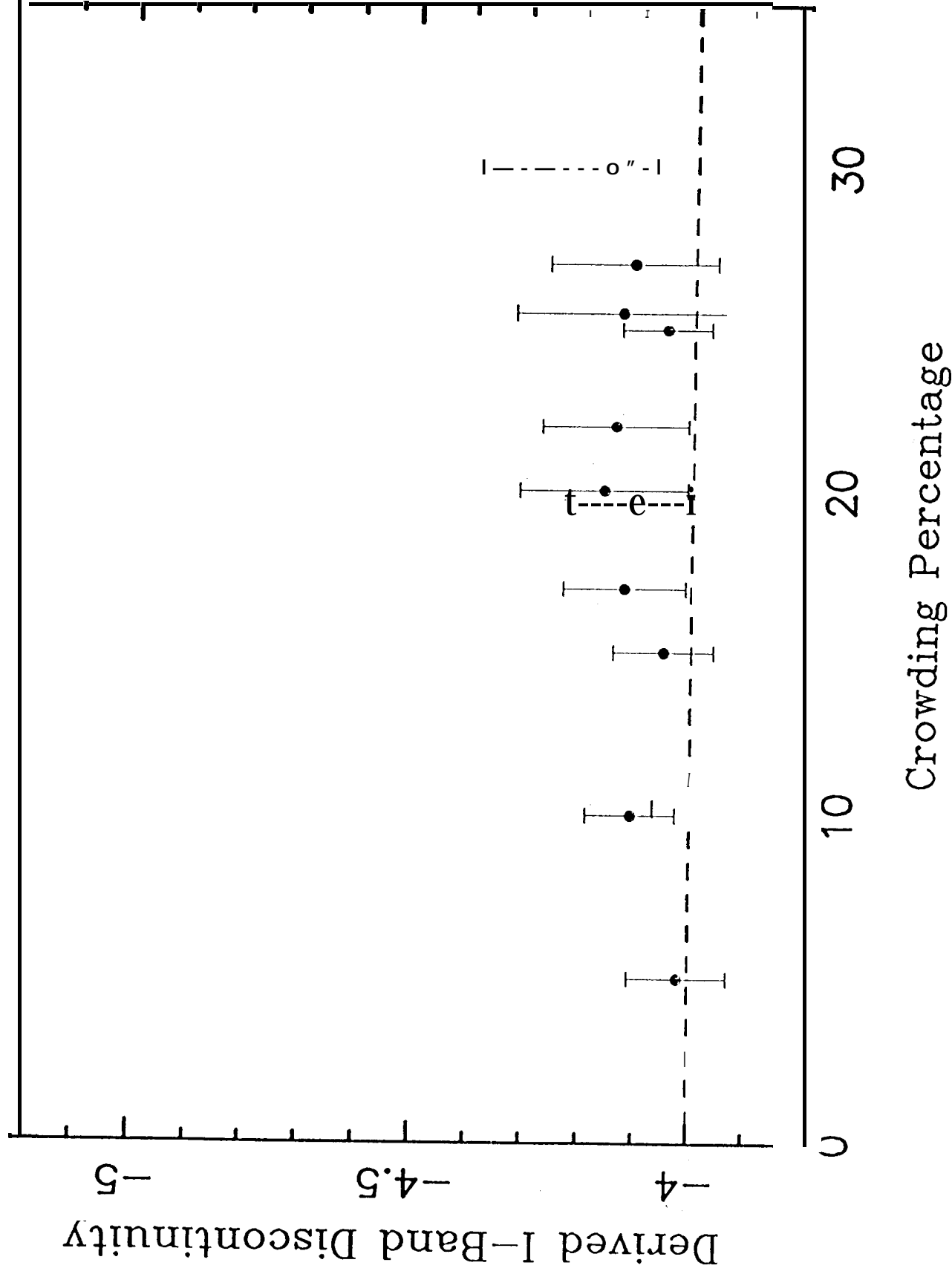
Red-Giant-Branch Color-Magnitude Diagram



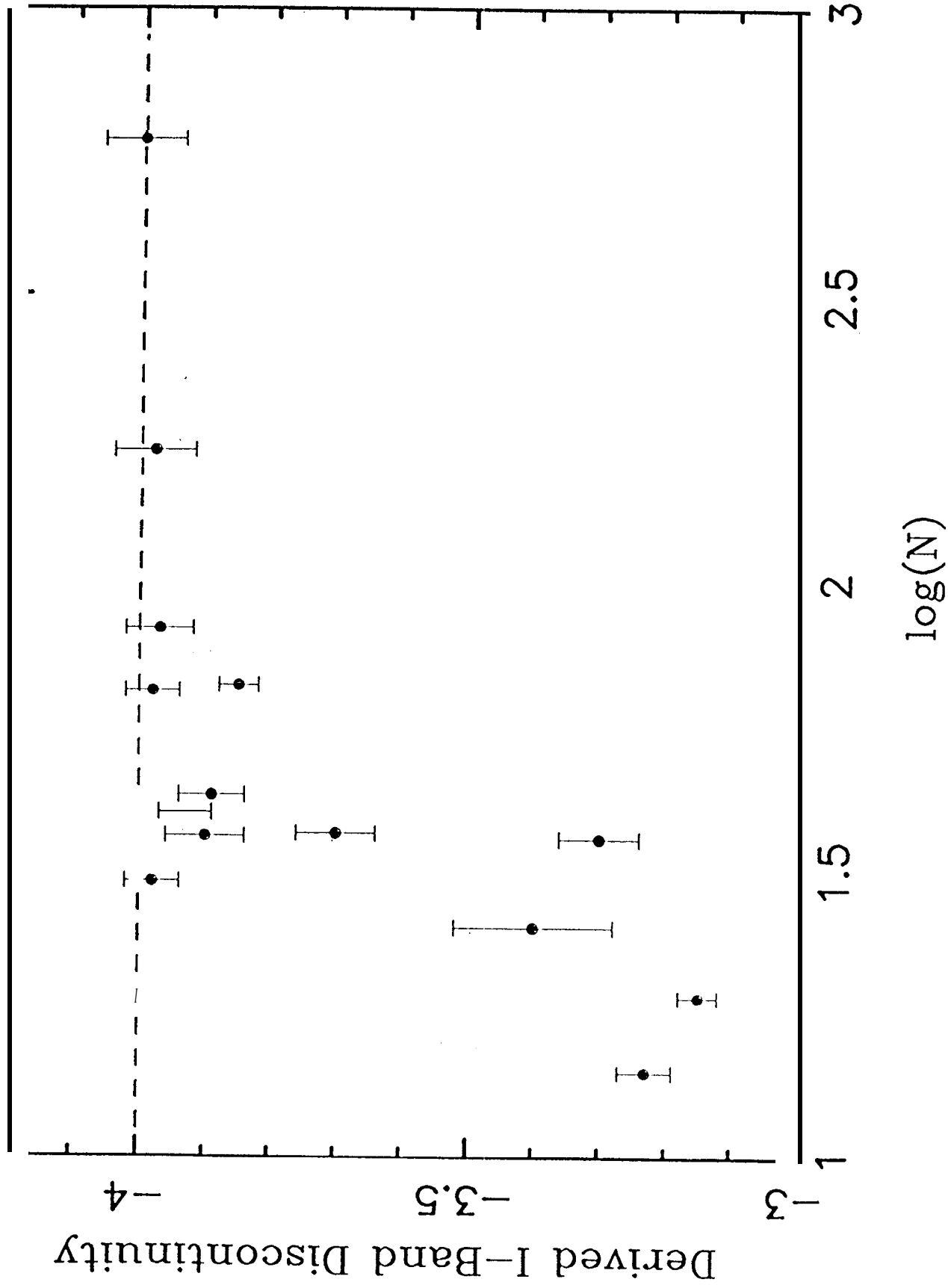
Edge Detection (2- and 4-Point Sobel Kernels)



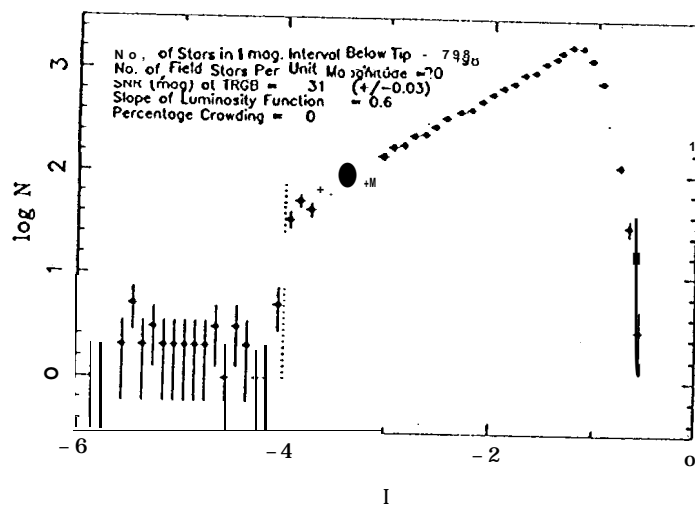
Systematic Effects of Crowding



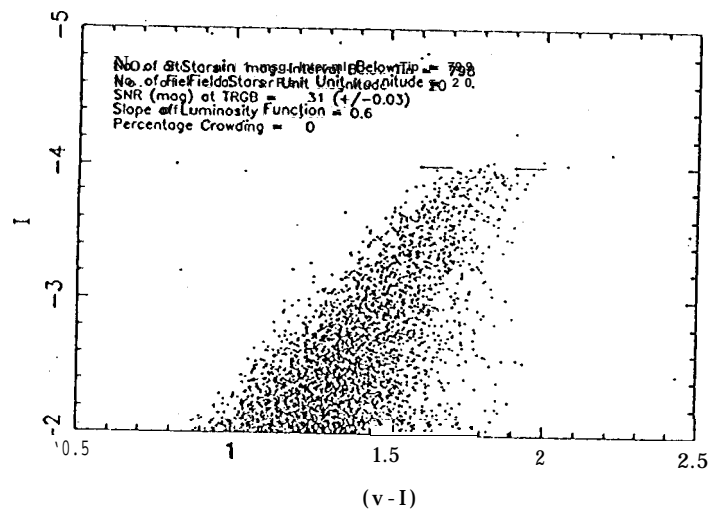
Systematic Effects of Population Size



I-Band Red-Giant-Branch Luminosity Function



Red-Giant-Branch Color-Magnitude Diagram



Edge Detection (2- and 4-Point Sobel Kernels)

